Received: 20 October 2021 | Revised: 13 June 2022 | Accepted: 28 June 2022

DOI: 10.1002/ep.13940

ENVIRONMENTAL PROGRESS & SUSTAINABLE ENERGY

ORIGINAL RESEARCH

Sustainable Energy

Catalytic role of binary oxides (CuO and Al_2O_3) on hydrogen storage in MgH_2

Ahammed Jubair[1] | Md. Akhlakur Rahman[1] | Md. Maksudur Rahman Khan[2] | Md. Wasikur Rahman[1]

[1]Department of Chemical Engineering, Jashore University of Science and Technology, Jashore, Bangladesh

[2]Faculty of Chemical and Process Engineering Technology, Universiti Malaysia Pahang, Gambang, Pahang, Malaysia

Correspondence
Md. Wasikur Rahman, Department of Chemical Engineering, Jashore University of Science and Technology, Jashore 7408, Bangladesh.
Email: w.rahman@just.edu.bd

Abstract

Hydrogen sorption characteristics of magnesium hydride (MgH_2) were enhanced by ball milling for 12 h under an inert atmosphere with the addition of 20 wt% Al_2O_3 and as prepared CuO. X-ray diffraction (XRD) characterization and thermal gravimetric analyzer coupled with a mass spectrometer (TGA-MS) of the ball milled samples were carried out to determine the H_2 sorption reactions. Additionally, XRD data were analyzed using Rietveld method to identify the crystallographic properties. Ball milled MgH_2 with β and γ allotrope mixtures were found with broad peaks in XRD indicating the as prepared samples are amorphous and strain, alongside bare additives. H_2 sorption in MgH_2 is greatly enhanced by the presence of CuO and Al_2O_3 binary oxides. TGA experiment demonstrated fast desorption kinetics for ball milled samples with the oxide additives. Particularly, MgH_2 milled with CuO showed a more remarkable effect on desorption kinetics rather than Al_2O_3. It takes less than 10 min to desorb more than 5 wt% H_2 at 623 K. The activation energy of H_2 desorption was estimated for the mixtures by Kissinger method and the lowest value (65 kJ mol^{-1}) was obtained for the MgH_2/CuO mixture. A kinetic model has been proposed in the context to illustrate the complex mechanism of dehydrogenation of MgH_2 with the additives. Finally, the addition of metal oxides influences H_2 sorption characteristics of MgH_2 through lowering the activation energy and reducing the waste of energy for diffusing the thin layer of Mg that creates a pathway to store H_2 within the system.

KEYWORDS
activation energy, ball milling, H_2 sorption, hydrogen storage, kinetics, magnesium hydride

1 | INTRODUCTION

Global clean energy demand is increasing inevitably followed by some consequences such as fossil fuel scarcity, environmental challenges, technological boundaries and infrastructure adjustment. Lately, considerable efforts have been made on the advancement in hydrogen storage materials mostly focused on lightweight and clean energy carriers for automobile applications. There are different types of methods for hydrogen storage, such as compressed hydrogen in a cylinder, liquid, stationary, automotive onboard hydrogen, and so forth. Hydrogen gas has a good energy density by weight; however, it has a low energy density by volume versus hydrocarbons. Therefore, it requires a large tank to store. A small hydrocarbon tank can hold an equal amount of energy that a large hydrogen tank does. To power the compressor, cylinder hydrogen costs 2.1 times the energy content. Without energy recovery, the higher compression means more energy lost in the compression step ('According to the dispersion model of hydrogen permeation for safety engineering and risk

assessment, 2009'). In the hydrogen tanks used in vehicles, hydrogen is compressed at 350–700 bar based on type IV carbon-composite technology ('fuel cell electric vehicles and hydrogen infrastructure: status 2012'). Car manufacturers, such as Honda (FCX Clarity) or Nissan (X-TRAIL FCV 03 model) are working on the subject matter to resolve this challenge.

Liquid hydrogen is used in the space shuttle. Massive energy loss occurs in liquefaction as liquid hydrogen needs cryogenic storage and its boiling point is only 20.268 K. The storage tank needs insulation to stop boiling, which increases operation cost. Comparing hydrocarbon fuels, liquid hydrogen provides less energy density by volume. Hydrogen can be used in the automobile as an alternative to fossil fuel and a car manufacturing company of BMW has started their work on the development of a liquid hydrogen storage tank (e.g., BMW Hydrogen 7). Japan has progressed greatly in the area of hydrogen storage and they already set up tanker ports with the capacity of storing liquid hydrogen (LH_2) in Kobe. It was expected that in 2020, they would receive their first shipment of LH_2 through the specially designed carrier. Hydrogen is liquefied by decreasing its temperature, as its critical temperature is about 33.19 K, almost similar to that of liquefied natural gas (LNG) which is stored at 111 K. It has been found that 12.79% of efficiency losses happened or specific energy of 4.26 kWh/kg out of 33.3 kWh/kg can be obtained.[1] An analysis of the main criteria of solid-state hydrogen storage families, according to the Department of Energy (DOE) for the onboard application is under consideration.

Intermetallic hydrides are essential for various applications of hydrides, and as a host, their properties are discussed in a detailed view. There are various types of intermetallic compounds practiced worldwide, for example, binary, ternary, quaternary, and more complicated systems. Molecular ratio and crystal analysis point out the fact that binary hydrides have considerable interlinear distance in size. For intermetallic compounds, when the electrons transfer from large electronegative molecules, more shrinkage in the unit cell occurs. This charge transfer is significant for the host material as it changes the density of the local electrons, which is counted as an essential factor for kinetics during hydrogen storage. The possible sites for hydrogen storage are either tetrahedral or octahedral structures inside a host metal. Considering thermodynamic and hydrogen storage properties of different binary hydrides, the best of them are summarized in Table 1.[2]

TABLE 1 Thermodynamic and hydrogen storage characteristics of some binary hydrides.[2,3]

Hydride	ΔH_n (kJ mol^{-1})	H_2 (wt%)	H_2 density (gl^{-1})
LiH	−180	12.7	98
BeH_2	19.3	18.2	118
MgH_2	−74	7.7	109
AlH_3	−8	10.1	149
ZrH_2	−163	2.2	123
NbH_2	−83	2.1	138
VH_2	−34	1.9	103

Considering environmental and economic parameters, a long-term vision of hydrogen storage application has been taken by DOE. Additionally, it has been predicted that at a temperature range of 60–120°C the minimal hydrogen storage capacity should be 6.5 wt% and 65 gl$^{-1,}$ and that will be commercially viable.[3] Therefore, AlH_3 and BeH_2 are better choices due to thermodynamic (−8 and 19.3 kJ mol^{-1}) and storage capacity (10.1 and 18.2 wt%) standpoints in comparison to other hydrides; however, they suffer drawbacks from H_2 desorption kinetics, availability, toxicity, and so forth.

On the contrary, MgH_2 is an excellent H_2 storage material used worldwide because of its convenient storage properties. It is highly abundant in earth crust that is approximately 2% and virtually unlimited in seawater,[4] nontoxic, low cost for large scale production with good reversibility[2,5] and it has relative safety of operation. MgH_2 has a significant advantage as it contains high volumetric (0.11 kg H_2l^{-1}) and gravimetric (7.7 wt% H_2) capacity. Nonetheless, the challenges of unsuitable thermodynamic properties, low kinetics, massive changes in volume during hydrogen sorption cycles, and highly explosive features have greatly hindered its practical applications.[6,7]

To improve hydrogen storage kinetics in MgH_2, numerous methods have been developed, such as ball milling, catalysis, surface modification, and so forth. Different catalysts/additives are employed to enhance the kinetics of MgH_2 such as transition metal oxides, alkali metal oxides, binary oxides, ternary oxides, alloys, nanocrystalline particles, nonmetallic catalysts, charcoal, and so forth. Recently, nanocatalysis draws immense attention to researchers as it increases the surface area of the catalysts to facilitate hydrogen sorption properties of the system. Hydrogen absorption and desorption characteristics of ball milled Mg-based hydrides with binary oxides are displayed in Table 2. It can be revealed from the table that most of the binary oxides were added (10 wt%) to the MgH_2 system to desorb H_2 (maximum capacity 3–5 wt%) for 60 min at sorption temperature (T_{abs} and T_{des} 300°C) and pressure (P_{abs} 10 bar) still a challenge to achieve the target of DOE.

Ball milling enhances the kinetics of hydrogen storage of MgH_2, and the use of transition metals and their oxides as catalysts/additives have added great contribution on desorption properties. For example, during the milling of β-MgH_2, the course form of SnO_2 powder was used as a lubricant, which reduces the quantity of γ-MgH_2 at the time of conversion. However, nanocrystalline SnO_2 powder has a very limited effect in decreasing the impact energy on MgH_2; while MgH_2 turn into γ polymorph through destabilizing and transformation. Similarly, Nb_2O_5, MoO_3 and Cr_2O_3 also have excellent catalytic properties which help to generate easy pathways for hydrogen diffusion thus enhances the hydrogen absorption and desorption in MgH_2.[7–9,11–13] Besides, it has been reported that H_2 sorption kinetics in MgH_2 can be improved by using multiple oxides[14] and more preferably ternary oxides as an alternative to single oxides.[13,15–20,21] Unfortunately, most of them used in these schemes suffer from higher calcination point, low activity and stability or high costs of metals. Therefore, the development of highly active, stable and cost effective catalysts that

TABLE 2 Hydrogen sorption characteristics of MgH_2 with different binary oxides.

Binary catalysts	Catalyst (%)	Temperature (°C) (T_{abs} and T_{des})	Pressure (bar) (P_{abs} and P_{des})	Kinetics (min)	Max H_2 (wt%)	References
Nb_2O_5	0.5 wt	300	8.4		7	[4]
CeO_2	10 wt	300	11	60	3.43	[8]
V_2O_5	10 wt	250 and 400	15	1.6 and 5	3.20	[8]
Al_2O_3	10 wt	300	11 and 0.5	60	5.66	[8]
Cr_2O_3	10 wt	300	11	60	5.87	[8]
CeO_2	10 wt	300	11	60	3.43	[8]
Al_2O_3	5 mol	300	15	67	4.49	[9]
Fe_2O_3	10 wt	300	12	60	5.56	[9]
Fe_2O_3	5 wt	300	2–15	20	1.37	[9]
TiO_2	10 wt	257	6	60	4.00	[10]

operate under mild conditions remains a challenge in the field of hydrogen storage.

Not much written in the literatures about copper oxide (CuO) synthesis and its application in H_2 desorption experiments. CuO nanoparticles were prepared in the current study by the chemical precipitation process and characterized by standard methods. Thereafter, the effect of binary oxides (CuO & Al_2O_3) on the H_2 sorption kinetics of MgH_2 has been explored to understand the catalytic effect of transition metal oxides. Structural properties of the solid-state materials were characterized by X-ray diffraction (XRD) and analyzed by Rietveld method as well as sorption kinetics, and activation energy for H_2 desorption of the ball milled MgH_2 were investigated with and without the addition of binary oxides. Finally, a kinetic model has been proposed in the context to elucidate the dehydrogenation mechanism of MgH_2 with the additives.

2 | EXPERIMENTAL

2.1 | Materials

The chemicals used in our research are laboratory standard and use without any further purification. Sodium hydroxide (NaOH) pellets and Aluminum oxide (Al_2O_3) were purchased from Lobha Chemie, India. Copper (II) chloride dihydrate ($CuCl_2$. $2H_2O$) was collected from Merck, India. Magnesium hydride was purchased from Langfang Bld Trade Co. Ltd, China. They were used after completed the XRD test without further purification. Copper oxide (CuO) nanoparticles were synthesized in the laboratory and characterized by standard methods. Aluminum oxide was collected from Merck, Germany, and used without any kind of purification.

2.2 | Materials preparation

The simple chemical precipitation process was used to produce CuO nanoparticles. Briefly, copper salt ('Copper chloride dihydrate') and the pellet of NaOH were dissolved in ethanol individually. Additionally, the NaOH solution was added dropwise to the mother solution (Copper chloride solution) at continuous stirring conditions and room temperature. The solution color will be turned black as the reaction finished and the precipitate settled at the bottom of the container. The precipitate was separated from the solution by using a centrifuge ('Eppendorf Refrigerated Centrifuge Model 5702R, Germany'). Then the precipitate was washed several times with DI water and ethanol, respectively to remove the unreacted chemicals and unwanted products. After washing them properly the as-prepared precipitate was dried in a vacuum drier at around 50°C. To obtain nanoparticles of different crystalline CuO, the dried particles were annealed at various temperatures of 200, 400, and 600°C. Furthermore, the annealed particles were grounded properly to get a fine powder of CuO. MgH_2 was milled in an inert environment with 20 wt% binary oxides (CuO and Al_2O_3) using a rotary ball mill (Fritsch P5). Five milligrams of the ground powder was taken in an 80 cm^3 of stainless steel vial with 26 stainless steel balls (Ø = 10 mm) during milling, where the ratio of powder weight to the ball was 1:24. Then the ball mill was operated for 1 h at a specific speed of 250 rpm and after 1 h the mill was kept at rest for 30 min to settle down the materials. This process of milling and resting the materials was repeated for 6 h to get a homogenous mixture.

2.3 | Materials characterization

The structure of as-prepared materials was analyzed by XRD at room temperature using an XRD diffractometer (Bruker D8 Advance) with a radiation source Cu-Kα, $\lambda = 0.15405$ nm, and XRD patterns were recorded in 2θ degrees from a range of 10–80° (40 kV, 40 mA, step size 0.020°, scan rate 4.01 min^{-1}). Specimen displacement correction is $T = 0.0043074$. A commonly used diffraction analysis program, the Rietveld refinement method was used to identify the crystallographic properties of the synthesized powder samples from the XRD patterns.[22] Dehydrogenation of the mixtures of MgH_2 with binary oxides was analyzed by thermal gravimetric analysis (TGA) using a TA

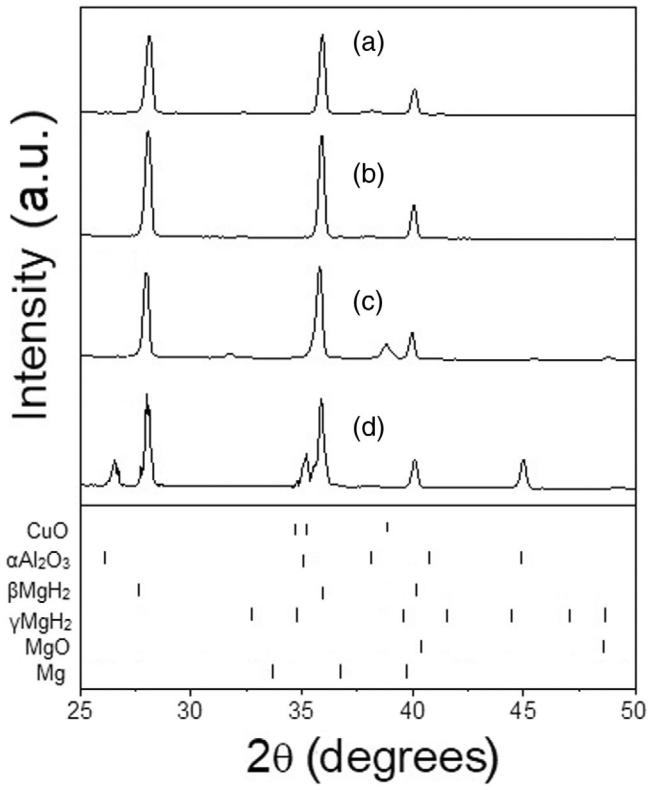

FIGURE 1 X-ray diffraction patterns of (a) fresh MgH_2, (b) ball milled MgH_2, (c) ball milled $MgH_2 + CuO$, and (d) ball milled $MgH_2 + Al_2O_3$

instrument (SDT600) coupled with a hidden analytical HPR-20 mass spectrometer (MS). Samples were heated at a certain temperature of 600°C with a constant flow of Ar gas; while the heating rate was maintained at 10°C min^{-1} for the first batch. To get the activation energy of dehydrogenation of MgH_2 some other samples were also heated with various heating rates of 20, 30, and 40°C min^{-1} which aids to develop Kissinger plots as well.

3 | RESULTS AND DISCUSSION

3.1 | XRD analysis

The as-prepared CuO nanoparticles were characterized by various methods reported in our previous works[23,24] and elsewhere.[25,26] The synthetic techniques might differ from the current study; nevertheless, the properties of the final product are analogous. After the synthesis, an almost pure compound has been obtained. Ball milled MgH_2 with CuO and Al_2O_3 additives lead to a microstructure refinement as shown in Figure 1b–d. Fresh MgH_2 is demonstrated as a reference for the others (Figure 1a). It was also noticed that the milled sample contains some MgH_2 of γ phase (orthorhombic) along with that of β phase (tetragonal). The formation of this phase is due to the ball milling and it is stable at high pressure.[27] Additionally, a considerable amount of MgO is usually formed (more than 10 wt%) because of the oxidation of Mg at the time of milling of MgH_2. Furthermore, Figure 1b–d displays the XRD patterns of the ball milled MgH_2 with additives producing broader peaks which confirm the smaller crystal size. After ball milling, the average crystal size of MgH_2 was obtained around 50 nm; while the size of the additives was found to be approximately 60–70 nm.

The size of the milled crystallite samples was reduced by ~90%. The comprehensive properties such as lattice constants, composition, and parameter of the microstructure of the milled samples are shown in Table 3 as obtained from the Rietveld refinement with excellent fittings (R = 3%–6%). In all the cases, the lattice constants of ball milled samples are comparable to those of as-received materials as well as reported in the crystallographic database, for example, the lattice constants of MgH_2 (ICSD-01-074-0934, a_0 = 4.5168 Å, and c_0 = 3.0205 Å). Binary oxides of 20 wt% were added to the system. Theoretical phase fraction of the additives for the various mixtures is equal to 17 and 18 wt% for the CuO and Al_2O_3 samples, respectively. Al_2O_3 being a trigonal crystal system occurs naturally in its crystalline polymorphic phase α-Al_2O_3 as the mineral corundum. Interestingly, the as-produced γ-Al_2O_3 is similar to the tetragonal structure instead of the generally adopted cubic structure which is confirmed by the splitted XRD peaks. Besides, the formation of α-alumina and γ-alumina is governed by the partial pressure of oxygen.[28,29] According to the results of the Rietveld analysis (Table 3), the relative amount of additives remains almost unchanged after milling suggests that additives undergo no reaction with MgH_2. These outcomes are also comparable to our previous study regarding ball milling of MgH_2 with various Mg-Nb-O ternary oxides.[30]

3.2 | TGA-MS analysis

To measure the dehydrogenation onset temperature and the amount of hydrogen desorption from the system, TGA-MS measurements were carried out for the ball milled samples as shown in Figure 2. The weight losses of milled MgH_2 with different binary oxides were found to be 5.8 wt% for Al_2O_3 and 6.4 wt% for CuO in comparison to those of fresh MgH_2 and ball milled MgH_2 corresponded to 6.6 and 6.8 wt%.

These values are very similar to the anticipated capacity reduction due to the reaction barrier of water and $Mg(OH)_2$. The addition of binary oxides with MgH_2 showed remarkable dehydrogenation properties. During dehydrogenation, the onset temperature of ball milled MgH_2 reduced from 400 to 360°C regarding fresh MgH_2 point out the effect of milling. Moreover, CuO and Al_2O_3 added ball milled mixtures reduced the temperature significantly from 400 to 260 and 310°C, respectively. From the desorption experiments, it was found that fresh MgH_2 desorbed H_2 about 5 wt% at 623 K for 30 min and more than 6.5 wt% desorbed at 648 K after 15 min; whereas, milled MgH_2 desorbed H_2 up to 2 wt% only at 573 K for 30 min and up to 6.8 wt% at 623 K after 15 min (Figure 2 and Table 4). MgH_2 milled with CuO showed more remarkable effect in desorption kinetics rather than Al_2O_3 as it took less than 10 min to desorb more than 5 wt% H_2 at 623 K. Additionally, the comparison of catalytic

TABLE 3 X-ray diffraction parameters derived from the diffraction patterns of fresh MgH_2, ball-milled MgH_2, ball-milled MgH_2/CuO, and ball-milled MgH_2/Al_2O_3 using Rietveld method.

			Lattice constants (Å)					
Ball milled samples	**Phase**	**wt%**	***a***	***b***	***c***	**Crystallite size (nm)**	**Micro strain**	***R*%**
Fresh MgH_2	β-MgH_2	94	4.5128	–	3.0236	240	6.0E−4	4.8
	Mg	6	3.2128	–	5.2192	250	1.0E−3	
Ball milled MgH_2	β-MgH_2	70	4.5132	–	3.0216	30	2.0E−3	3.4
	γ-MgH_2	16	4.5031	5.4197	4.9128	35	8.0E−4	
	Mg	5	3.2158	–	5.2122	50	9.0E−4	
	MgO	9	4.2268	–	–	15	8.0E−4	
Ball milled MgH_2/CuO	β-MgH_2	68	4.5156	–	3.0291	35	3.0E−3	6.04
	γ-MgH_2	5	4.5055	5.4197	4.9166	35	8.0E−4	
	CuO	17	4.6893	3.4268	5.1321	60	1.32E−3	
	Mg	5	3.2126	–	5.2109	45	2.0E−3	
	MgO	5	4.221	–	–	20	8.0E−4	
Ball milled MgH_2/Al_2O_3	β-MgH_2	67	4.5169	–	3.0296	30	2.0E−4	5.62
	γ-MgH_2	6	4.5194	5.4256	4.919	40	8.0E−4	
	Al_2O_3	18	14.1941	5.7035	5.0392	107	3.7E−4	
	Mg	3	3.2462	–	5.2393	25	1.0E−2	
	MgO	6	4.2277	–	–	60	8.0E−4	

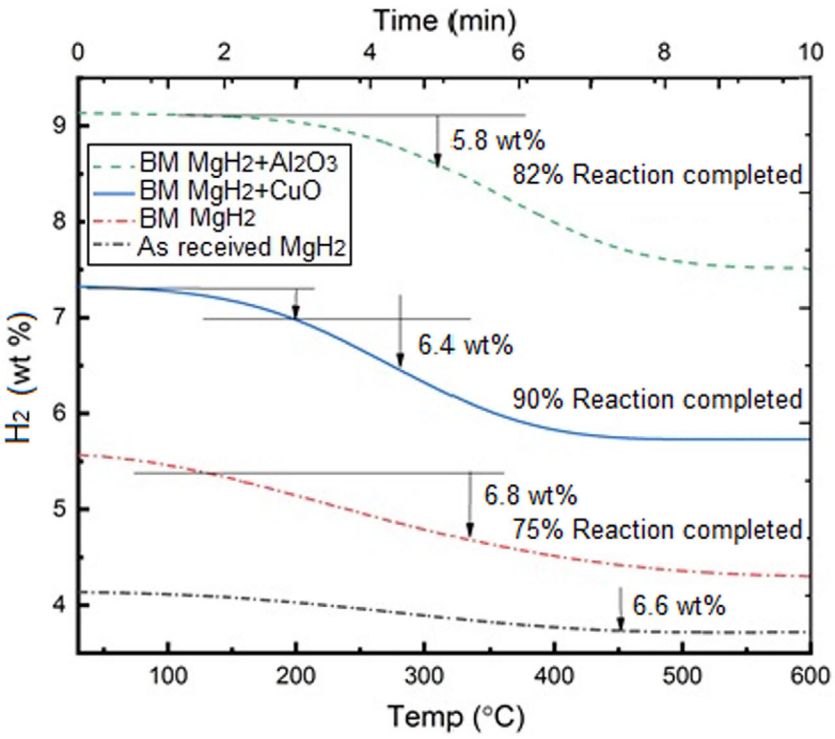

FIGURE 2 Stacked thermal gravimetric analyzer coupled with a mass spectrometer plots of H_2 desorption at different temperatures of fresh MgH_2, ball milled (BM) MgH_2, BM MgH_2/CuO, and BM MgH_2/Al_2O_3.

performance of different materials used for hydrogen gas storage is shown in Table 5.

After analyzing the effect of additives on the dehydrogenation of MgH_2, it has been observed that binary oxides have a progressive influence on decreasing the onset temperature. Besides, the particle size of the binary oxides on catalytic activity is also a pivotal factor in dropping the onset temperature. The ball milling process makes defects on the surface of the materials and these defects create more space to store H_2 inside as well as require a short time to discharge. Ball milled MgH_2/CuO showed a better result than the others might be due to the higher catalytic effect and smaller particle size that dispersed in MgH_2 during milling. Al_2O_3 showed a decent catalytic

impact with a lower dehydrogenation temperature than milled MgH_2. In comparison to different binary oxides, CuO demonstrated lower dehydrogenation temperature with efficient time coverage. The presence of CuO may assist the formation of ternary oxides which can be explained by thermodynamic argument. The addition of CuO and Al_2O_3 possibly reacts with surface MgO results in the formation of ternary oxides (Mg-Cu-O and Mg-Al-O), thereby decreasing the appearance of non-permeable MgO. CuO nanoparticles can be incorporated on the surface of MgH_2 at the time of ball milling. Furthermore, the CuO does not undergo any destruction or react with Mg. It is also not reduced or dissolved on the Mg surface at the time of dehydrogenation proved by the analysis of XRD results. The CuO nanoparticles are more favorable as compared to Al_2O_3 because of their Gibbs free energy (623 K).[18,38] This might be the main cause that CuO is usually not reduced during milling with MgH_2. These properties of CuO help to convert MgO to Mg-Cu-O rather than Mg-Al-O. The solid–solid reactions between different polymorphs of alumina and MgO generally happened at different temperatures. The ease of response follows the order of amorphous alumina > γ-alumina > α-alumina.

In fact, the combined effect of metal oxides and milling largely reduce the hydrogen desorption temperature of MgH_2. It was reported that the combined effect of SnO_2 reduced the hydrogen desorption temperature by 60 K and stabilized the MgH_2. The sorption characteristics of MgH_2 powder can be enhanced by the use of Fe and its oxides (Fe_2O_3 and Fe_3O_4) as catalysts. During ball milling, these catalysts are homogeneously dispersed in the matrix of hydride that significantly improves the hydrogen sorption kinetics.[3] Similarly, MoO_3 also has excellent catalytic properties which help to generate easy pathways for hydrogen diffusion thus enhances the hydrogen absorption and desorption in MgH_2. It has been observed that during the hydrogenation process, MoO_3 converted to MoO_2 as a result the catalytic activity is decreased. This type of activity symbolizes the higher catalytic properties of MoO_3 during dehydrogenation.[11] In the improvement of hydrogen sorption activity in MgH_2, transition metals and their oxides have a great contribution during ball milling. Particularly, Nb_2O_5 and Cr_2O_3 have recently attracted considerable interest in the field.[7–9,12,13] The milling of MgH_2 with Nb_2O_5 powder dramatically reduces the hydrogen sorption time as well as enhances the kinetics of the reaction. However, all transition metals and their oxides are not equally suitable as additives due to their different physical and chemical properties. In fact, the activity of additives and catalysts also greatly depends on the conditions of ball milling.[12] Still now, most of the researches on H_2 storage is mainly focused on the effects of single oxides and optimized their amount to enhance the storage activity of MgH_2.

Additionally, H_2 sorption kinetics in MgH_2 can be enhanced by the use of multiple oxides instead of single oxides. According to the previous report, the combined use of ZnO/Nb_2O_5 and Cr_2O_3/Nb_2O_5 increased the sorption activity of MgH_2 effectively than the use of single oxides.[14] Moreover, it was explored that the use of multiple oxides such as $Nb_2O_5/Cr_2O_3/Al_2O_3$ generates synergistic effects to form ternary oxides, which significantly improves the hydrogen sorption kinetics in MgH_2. We reported earlier that as-prepared ternary Mg-Nb oxides (e.g., $MgNb_2O_{3.67}$) showed higher H_2 desorption properties than that of single Nb_2O_5 binary oxide.[39] This usually happens due to the synergistic effects between metal oxides and MgH_2. Furthermore, improvement in the kinetic reaction of H_2 desorption has been explained by the addition of ternary oxides, which is preferable than single or multiple oxides.[13,15–20]

An additional concern of ball milled MgH_2 as it may react with moisture present in reactive vial via spontaneous reaction:

TABLE 4 The effects of onset temperature on the dehydrogenation kinetics fresh MgH_2 and ball milled (BM) MgH_2, BM MgH_2/CuO, and BM MgH_2/Al_2O_3.

Sample	Onset temperature (°C)	Dehydrogenation kinetics
Fresh MgH_2	450	Very slow kinetics
BM MgH_2	356	75% complete in 10 min
BM MgH_2/CuO	280	90% in 10 min
BM MgH_2/Al_2O_3	310	81% in 10 min and 90% in 15 min

TABLE 5 Comparison of catalytic performance of different materials used for hydrogen storage.

Storage materials	Temperature (K)	Pressure (MPa)	Desorbed H_2 (wt%)	References
$CaMg_2$ and $CaMg_{1.9}Ni_{0.1}$ alloy	573	3.8	4.48	[31]
Li_2TiO_3 doped MgH_2	473	2.5	6.9	[32]
$Ba_2Mg_7H_{18}$	653	8	4	[33]
MgH_2-nfTa_2O_5 composite	373	2	6	[34]
$CeH_{2.73}$ and Ni in $CeH_{2.73}$-MgH_2-Ni Nanocomposites	505	3.5	4	[35]
Mg_3Pr and $Mg_3PrNi_{0.1}$ alloys	298	3.5	3.23	[36]
Mg-Ni/Mm-Ni multi-layer film	593	–	5.2	[37]
$Mg_3LaNi_{0.1}$	530	3.5	2.73	[38]
$MgCuO_2/MgAl_2O_4$	623	–	>5	This work

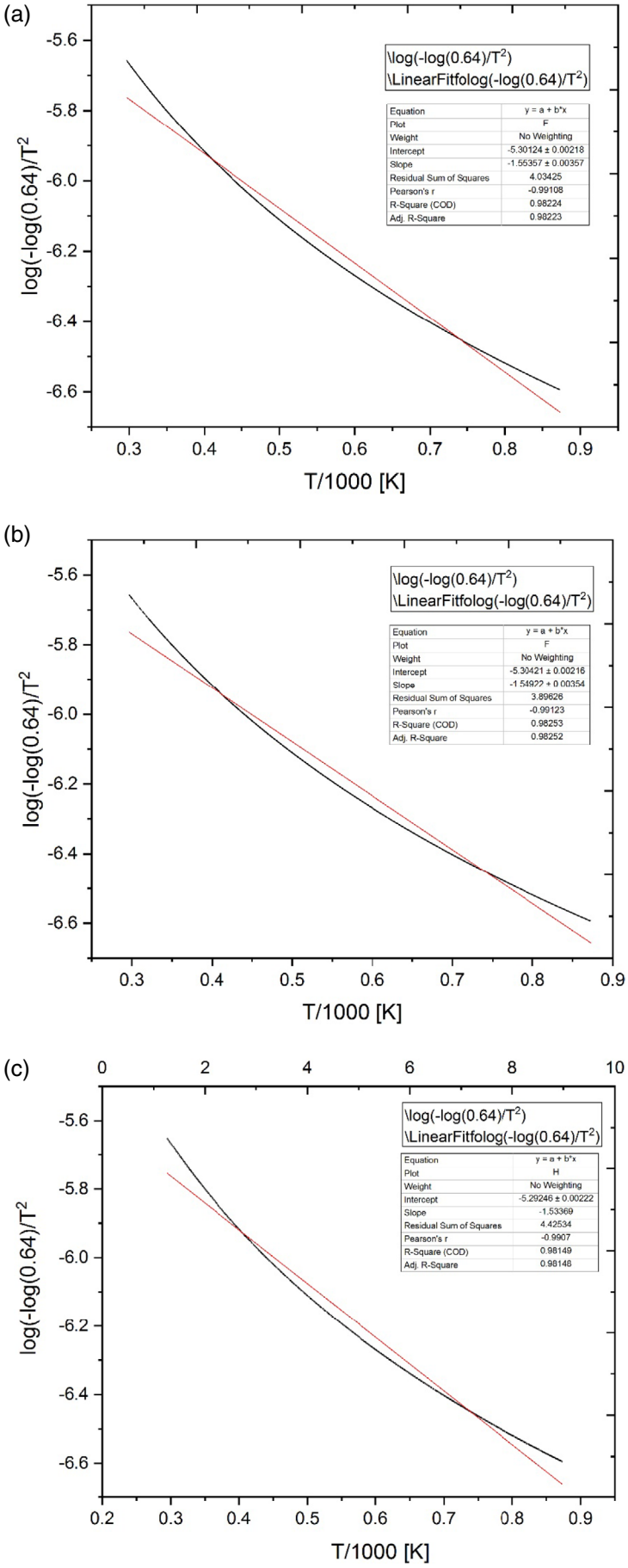

FIGURE 3 Thermal gravimetric analyzer coupled with a mass spectrometer (TGA-MS) plots of activation energy calculation by Kissinger equation. (a) Fresh MgH_2. TGA-MS plots of activation energy calculation by Kissinger equation. (b) ball milled MgH_2. TGA-MS plots of activation energy calculation by Kissinger equation. (c) ball milled MgH_2/CuO

$$MgH_2 + 2H_2O = Mg(OH)_2 + 2H_2 \Delta H = -277\,kJ\,mol^{-1}.$$

This reaction decreases the maximum nominal hydrogen storage capacity of MgH_2 by creating a layer of $Mg(OH)_2$. Besides, MgO negatively affects the H_2 desorption capacity and sorption kinetics by forming an impermeable oxide layer on the MgH_2 surface. A trivial contact of air may create this layer on MgH_2 and additional energy (-277 kJ mol^{-1}) is required to break down the coating to release H_2 suitably as well as generates problems in H_2 sorption cycles. MgO was traced in XRD results (5–10 wt%) obtained by the Rietveld method; whereas, $Mg(OH)_2$ did not show any remarkable peak indicating a trace amount of hydroxide might present in the samples.

Moreover, a small amount of metallic Mg, Cu, and Al might be presented in the ball milled samples; however, Cu and Al were not traced in the Rietveld refinement. These elements might be reduced to lower oxidation states due to rising temperature during milling. The Gibbs free energy (ΔG) of oxidation of Mg, Cu, and Al at 298 K are given below.[40]

$$2Mg + O_2 = 2MgO \qquad \Delta G = -1141\,kJ\,mol^{-1}.$$

$$Cu + O_2 = CuO \qquad \Delta G = -307\,kJ\,mol^{-1}.$$

$$Al + O_2 = Al_2O_3 \qquad \Delta G = -1582.3\,kJ\,mol^{-1}.$$

These reactions possibly occur during the dehydrogenation of MgH_2 at elevated temperatures. Therefore, the dehydrogenation rate may reduce simultaneously on repeated cycles. Kissinger strategies were constructed to figure out the activation energy of the MgH_2 systems by plotting the log of different heating rates over maximum peak temperatures against the inverse of the peak temperatures from the data of TGA-MS (Figure 3).

It has been revealed from the experimental results that activation energy of the commercially available MgH_2, ball milled MgH_2/CuO, and ball milled MgH_2 were obtained approximately 142, 65, and 129 kJ mol^{-1}, respectively (Figure 3b,c). The TGA-MS experiments were used to identify the activation energy at different rates of heating which indicates that less activation energy is required for MgH_2/CuO comparing to other metal oxides. During the current investigation, fresh MgH_2 has an activation energy of around 142 kJ mol^{-1} (Figure 3a) and after ball milling, it decreased to 129 kJ mol^{-1} (Figure 3b). Al_2O_3 and CuO additives demonstrated these values of nearly 93 and 65 kJ mol^{-1}, respectively (Figure 3c). These results are comparable to those extensively studied additives of TiO_2 showed around 72 kJ mol^{-1} and Nb_2O_5 63–83 kJ mol^{-1}.[28] The highest result was attained with a mixture of MgH_2 and 20 wt% SnO_2 and this mixture reduced the hydrogen desorption activation energy from 175 to 149 kJ mol^{-1} and the hydrogen storage capacity was also enhanced to 6.8 wt%.[18]

According to the previous results, it is clear that the incorporation of additives with MgH_2 enhanced the H_2 desorption reaction kinetics and reduce the relative amount at the time of response results. The proposed pathway effects are supported by this analysis for H_2 absorption and desorption in Mg,[5] and the reduced oxidation state represents the activity of Nb(V) in Nb_2O_5. It is noticeable that hydride mixtures of metal oxides (e.g., CuO and Al_2O_3 in the current study) with lower oxidation states can enhance the H_2 penetration through the layer of MgO. $Mg_3Nb_6O_{11}$ compound other than single oxides (e.g., MgO and Nb_2O_5) having reduced oxidation state was considered as more active for H_2 absorption with respect to Nb(V) based compounds at low pressure.[17,29,41] Moreover, reversible interaction of H_2 with the oxides largely depends on the crystal structure of the solid material such as the existence of octahedral crystal structure in the solid oxide. The octahedral crystals present in CuO and Al_2O_3 lattices

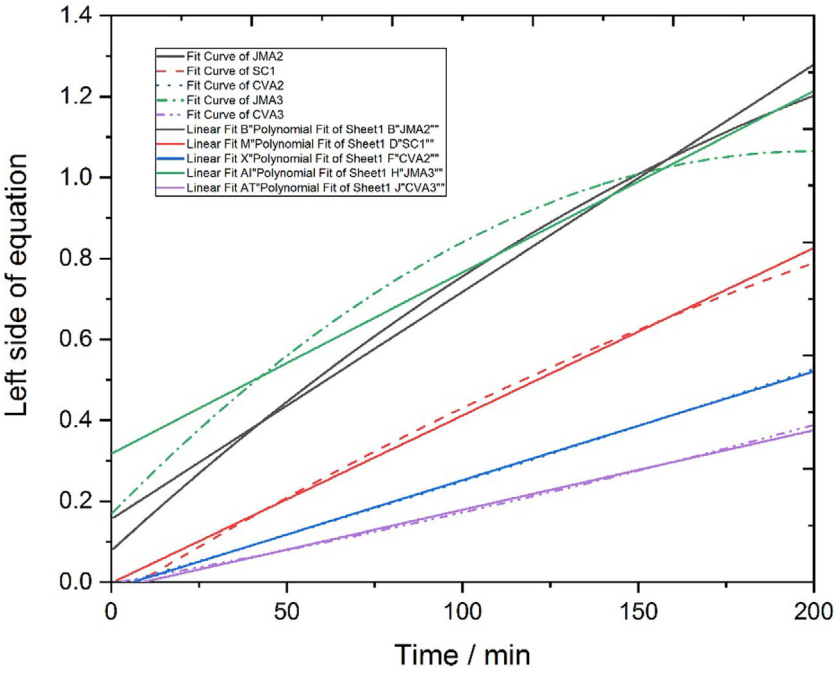

FIGURE 4 Curve of dehydrogenation kinetics for ball milled MgH_2.

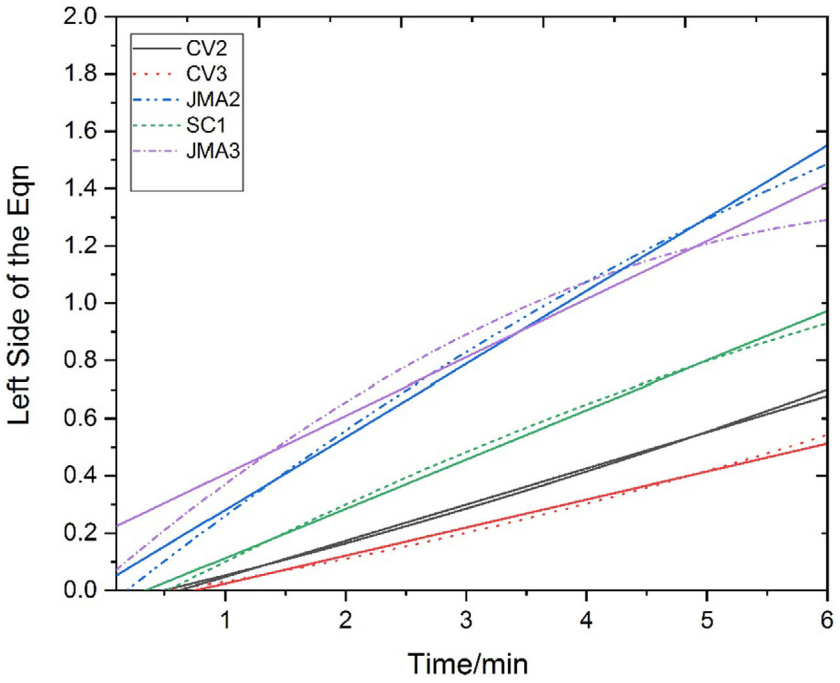

FIGURE 5 Curve fitting of dehydrogenation kinetics for ball milled MgH_2/CuO.

contribute to ameliorate sorption kinetics. The role of copper and aluminum is like niobium which acts as active sites for hydrogen desorption results in a quick sorption reaction with the addition of metal oxides.[41] The effect of magnesium niobates (Mg-Nb-O) on MgH_2 was reported elsewhere.[15,16] Our group studied earlier the effect of binary (Nb_2O_5) and ternary (Mg-Nb-O) oxides on H_2 absorption and desorption concluded that the catalytic role of ternary oxides is predominant.[13,17,18] According to the model of the reactive pathways, Nb_2O_5 converted to metallic Nb at the time of reduction. Additionally, the ternary phase of Mg-Nb-O of different stoichiometry also forms at the surface of MgH_2 which then improves the sorption properties of hydrogen.[19] MgH_2 can be destabilized by using metal oxides resulting in the formation of δ-MgH_2 that interacts with the additives and forms non-permeable MgO layer outside the Mg particles.[20]

Many researchers have developed a number of models of reaction kinetics. These mechanisms help to explain the dehydrogenation mechanism of MgH_2 along with metal oxide additives.[28] Rahman et al. studied a kinetic model for the MgH_2-Nb_2O_5 system.[17] These models are also applicable in this study based on TGA-MS data of the ball milled MgH_2 (Figure 4) and ball milled MgH_2/CuO system (Figure 5). The models can be explained by the following equations (Table 6).[9]

Here α is the transformed phase fraction, k and t symbolize the rate of reaction and reaction time, respectively. Equation (1) in Table 5 represents the surface-controlled reaction (SC1) and in this case, the rate-limiting step is the recombination of hydrogen into dihydrogen. Additionally, nucleation growth of the bulk surface was described by the Johnson–Mehl–Avrami models (JMA2 and JMA3) as illustrated in Equations (2) and (3) in Table 5. These two equations describe the two-dimensional (JMA2) as well as the three-dimensional (JMA3) expansion of the nucleus. Considering the equations, the rate-determining step is the velocity of moving interfaces among metal oxides and hydrides. Similarly, Equations (4) and (5) in Table 5 indicate that at the first stage nucleation of the molecules originates on the surface followed by moving into bulk towards the core of the particles. MgH_2 with bare additives just milled out through the mechanical process did not fit with any design equation over the full-time analysis (Figure 4). Nonetheless, the closest model that works well with the CV2 model. According to this model, reaction kinetics is usually controlled by the movement of the interface among MgO present on the MgH_2 surface and the contacting hydride where two-dimensional interface growth occurred. Zaluska et al. proposed this interfacial growth ensued along with grain boundaries.[4] Different research groups have suggested the dehydrogenation mechanism of an initial surface-controlled reaction of milled MgH_2.[9] Nevertheless, there are no significant differences between the surface controlled model nor the CV2 and CV3 models as the dehydrogenation temperature rate is changed.

For MgH_2 milled with CuO, the JMA2 and JMA3 models are quite similar to the nucleation growth of Mg along with the grain boundaries within the bulk (Figure 5). This phenomenon expresses that

TABLE 6 Different kinetic model equations.

Sl. No.	Equation	Model indicator
1	$\alpha = kt$	SC1
2	$[-\ln(1-\alpha)]^{\frac{1}{2}} = kt$	JMA2
3	$[-\ln(1-\alpha)]^{\frac{1}{3}} = kt$	JMA3
4	$[1-(1-\alpha)]^{\frac{1}{2}} = kt$	CV2
5	$[1-(1-\alpha)]^{\frac{1}{3}} = kt$	CV3

lower energy is provided for grain boundaries during diffusion.[42] Consequently, it clarifies that CuO as additive influences to lower the activation energy of the grain boundary of MgH_2 as well as reduces the waste of energy for diffusing the thin layer of Mg and creates a way to diffuse the H_2 within a short time as well as limiting the point. It can be anticipated that TGA-MS data of Al_2O_3 follows the JMA2 and JMA3 models, but the nucleation growth is slower than CuO as the dehydrogenation temperature is higher as well. According to the previous report, MgH_2/Nb_2O_5 usually followed the kinetic model of two-dimensional nucleation growth of CV2[28]; but in this case, the JMA2 and JMA3 are more appropriate models to describe the two dimensional and three-dimensional interface growths. Different methods, along with various additives, support some other models. MgH_2-TiO_2 also follows the JMA2 and JMA3 models rather than CV2.[4]

4 | CONCLUSION

Hydrogen sorption reactions of ball milled MgH_2 with binary oxides (CuO & Al_2O_3) were studied successfully to understand the effect of multiple oxides (CuO/Al_2O_3) as well as ternary oxides ($MgCuO_2$/$MgAl_2O_4$) prepared by the single oxides. The H_2 desorption rate in MgH_2 is enhanced by the use of ball milled binary metal oxides. Additionally, CuO nanoparticles were prepared through the chemical precipitation method and found to be highly effective for the desorption reaction in decreasing the dehydrogenation onset temperature to around 250°C than the other samples. The mixtures of ball milled MgH_2/CuO and MgH_2/Al_2O_3 improve the hydrogen desorption significantly by lowering the activation energy besides the change in the reaction mechanism. A kinetic model has been proposed in the context to explain the complex mechanism of dehydrogenation of MgH_2 with oxide additives and compared them to those with bare additives. Hydrogen absorption/desorption properties of ball milled samples catalyzed by the as-prepared ternary oxides ($MgCuO_2/MgAl_2O_4$) from the binary oxides/multiple oxides (CuO/Al_2O_3 and surface MgO) will be studied in the forthcoming issues.

AUTHOR CONTRIBUTIONS

Ahammed Jubair: Data curation (equal); formal analysis (equal); investigation (equal); methodology (equal); software (equal); writing – original draft (equal). **Md. Akhlakur Rahman:** Data curation (equal); formal analysis (equal); investigation (equal); methodology (equal); software (equal); writing – original draft (equal). **Md. Maksudur Rahman Khan:** Conceptualization (equal); resources (equal); validation (equal); visualization (equal); writing – review and editing (lead).

ACKNOWLEDGMENTS

The authors acknowledge the contribution of ball milling in Bangladesh Council of Scientific and Industrial Research (BCSIR) and technical support of MENTECH Labs of Jashore University of Science and Technology.

DATA AVAILABILITY STATEMENT

The data that support the findings of this study are available from the corresponding author upon reasonable request.

ORCID

Md. Wasikur Rahman https://orcid.org/0000-0002-2443-1062

REFERENCES

1. Sadaghiani MS, Mehrpooya M, Ansarinasab H. Process development and exergy cost sensitivity analysis of a novel hydrogen liquefaction process. *Int J Hydrog Energy*. 2017;42(50):29797-29819. doi:10.1016/j.ijhydene.2017.10.124
2. Aguey-Zinsou KF, Ares-Fernández JR. Hydrogen in magnesium: new perspectives toward functional stores. *Energy Environ Sci*. 2010;3(5):526-543. doi:10.1039/b921645f
3. Young KH. Research in nickel/metal hydride batteries 2016. *Batteries*. 2016;2(4):1-5. doi:10.3390/batteries2040031
4. Yartys VA, Lototskyy MV, Akiba E, et al. Magnesium based materials for hydrogen-based energy storage: past, present, and future. *Int J Hydrog Energy*. 2019;44(15):7809-7859. doi:10.1016/j.ijhydene.2018.12.212
5. Sakintuna B, Lamari-Darkrim F, Hirscher M. Metal hydride materials for solid hydrogen storage: A review. *Int J Hydrogen Energy*. 2007;32(9):1121-1140. doi:10.1016/j.ijhydene.2006.11.022
6. Wiswall R. Hydrogen storage in metals. In: Alefeld G, Völkl J, eds. *Hydrogen in Metals II. Topics in Applied Physics*. Vol 29. Springer; 1978. doi:10.1007/3-540-08883-0_21
7. Fukai Y. *The Metal–Hydrogen System*. 2nd ed. Springer-Verlag; 2018.
8. Dan L, Hu L, Wang H, Zhu M. Excellent catalysis of MoO_3 on the hydrogen sorption of MgH_2. *Int J Hydrog Energy*. 2019;44(55):29249-29254. doi:10.1016/j.ijhydene.2019.01.285
9. Barkhordarian G, Klassen T, Bormann RU. Effect of Nb_2O_5 content on hydrogen reaction kinetics of Mg. *J Alloys Compd*. 2004;364(1–2):242-246. doi:10.1016/S0925-8388(03)00530-9
10. Li B, Li J, Zhao H, Yu X, Shao H. Mg-based metastable nanoalloys for hydrogen storage. *Int J Hydrog Energy*. 2019;44(12):6007-6018. doi:10.1016/j.ijhydene.2019.01.127
11. Patah A, Takasaki A, Szmyd JS. Synergetic effect of oxides on hydrogen reaction kinetics of magnesium hydride. *Mater Sci Forum*. 2007;561–565:1605-1608.
12. Dehouche Z, Klassen T, Oelerich W, Goyette J, Bose TK, Schulz R. Cycling and thermal stability of nanostructured MgH_2–Cr_2O_3 composite for hydrogen storage. *J Alloys Compd*. 2002;347(1–2):319-323. doi:10.1016/S0925-8388(02)00784-3
13. Bhat VV, Rougier A, Aymard L, Darok X, Nazri G, Tarascon JM. The catalytic activity of oxides and halides on hydrogen storage of MgH_2. *J Power Sources*. 2006;159(1):107-110. doi:10.1016/j.jpowsour.2006.04.059
14. Friedrichs O, Klassen T, Sánchez-López JC, Bormann R, Fernández A. Hydrogen sorption improvement of nanocrystalline MgH_2 by Nb_2O_5 nanoparticles. *Scr Mater*. 2006;54(7):1293-1297. doi:10.1016/j.scriptamat.2005.12.011
15. Patah A, Takasaki A, Szmyd JS. Influence of multiple oxide (Cr_2O_3/Nb_2O_5) addition on the sorption kinetics of MgH_2. *Int J Hydrog Energy*. 2009;34(7):3032-3037. doi:10.1016/j.ijhydene.2009.01.086
16. Friedrichs O, Sa JC, Lo C, Klassen T. Nb_2O_5 'pathway effect' on hydrogen sorption in mg. *J Phys Chem B*. 2006;110(15):7845-7850. doi:10.1021/jp0574495
17. Rahman MW, Livraghi S, Dolci F, Baricco M, Giamello E. Hydrogen sorption properties of ternary mg–Nb–O phases synthesized by solid-state reaction. *Int J Hydrog Energy*. 2011;36(13):7932-7936. doi:10.1016/j.ijhydene.2011.01.053
18. Rahman MW, Castellero A, Enzo S, Livraghi S, Giamello E, Baricco M. Effect of mg–Nb oxides addition on hydrogen sorption in MgH_2.

J Alloys Compd. 2011;509(1):S438-S443. doi:10.1016/j.jallcom.2011.02.064
19. Andreasen A, Sørensen MB, Burkarl R, et al. Dehydrogenation kinetics of air-exposed MgH_2/Mg_2Cu and $MgH_2/MgCu_2$ studied with in situ X-ray powder diffraction. *Appl Phys Mater Sci Process*. 2006;82(3):515-521. doi:10.1007/s00339-005-3423-x
20. Hanada N, Ichikawa T, Hino S, Fujii H. Remarkable improvement of hydrogen sorption kinetics in magnesium catalyzed with Nb_2O_5. *J Alloys Compd*. 2006;420(1–2):46-49. doi:10.1016/j.jallcom.2005.08.084
21. Inamuddin K, Abbas H. Ternary graphene@polyaniline-TiO_2 composite for glucose biofuel cell anode application. *Int J Hydrog Energy*. 2019;44(39):22173-22180. doi:10.1016/j.ijhydene.2019.06.153
22. Borgschulte A, Bösenberg U, Barkhordarian G, Dornheim M, Bormann R. Enhanced hydrogen sorption kinetics of magnesium by destabilized MgH_2-δ. *Catal Today*. 2007;120(3–4):262-269. doi:10.1016/j.cattod.2006.09.031
23. Lutterotti L, Matthies S, Wenk H, Schultz AS, Jr JWR. Combined texture and structure analysis of deformed limestone from time-of-flight neutron diffraction spectra. *J Appl Phys*. 2014;82(4):1997. doi:10.1063/1.364220
24. Ong HR, Khan MMR, Ramli R, Yunus RM, Rahman MW. Glycerolysis of palm oil using copper oxide nanoparticles combined with homogeneous base catalyst. *New J Chem*. 2016;40(10):8704-8709. doi:10.1039/c6nj01461e
25. Ong HR, Khan MMR, Ramli R, Rahman MW, Yunus RM. Tailoring base-catalyzed synthesis of palm oil-based alkyd resin through CuO nanoparticles. *RSC Adv*. 2015;5(116):95894-95902. doi:10.1039/c5ra19575f
26. Naika HR, Lingaraju K, Manjunath K, et al. Green synthesis of CuO nanoparticles using Gloriosa superba L. extract and their antibacterial activity. *J Taibah Univ Sci*. 2015;9(1):7-12. doi:10.1016/j.jtusci.2014.04.006
27. Phiwdang K, Suphankij S, Mekprasart W, Pecharapa W. Synthesis of CuO nanoparticles by precipitation method using different precursors. *Energy Procedia*. 2013;34:740-745. doi:10.1016/j.egypro.2013.06.808
28. Bobet JL, Kandavel M, Ramaprabhu S. Effects of ball-milling conditions and additives on the hydrogen sorption properties of Mg + 5 wt% Cr_2O_3 mixtures. *J Mater Res*. 2006;21(7):1747-1752. doi:10.1557/jmr.2006.0206
29. Abdellatief M, Campostrini R, Leoni M, Scardi P. Effects of SnO_2 on hydrogen desorption of MgH_2. *Int J Hydrog Energy*. 2013;38(11):4664-4669. doi:10.1016/j.ijhydene.2013.02.016
30. Hu W, Donat F, Scott SA, Dennis JS. The interaction between CuO and Al_2O_3 and the reactivity of copper aluminates below 1000°C and their implication on the use of the Cu–Al–O system for oxygen storage and production. *RSC Adv*. 2016;6(114):113016-113024. doi:10.1039/c6ra22712k
31. Ma M, Duan R, Ouyang L, et al. Hydrogen storage and hydrogen generation properties of CaMg2-based alloys. *J Alloys Compd*. 2017;691:929-935. doi:10.1016/j.jallcom.2016.08.307
32. Zhang T, Isobe S, Jain A, et al. Enhancement of hydrogen desorption kinetics in magnesium hydride by doping with lithium metatitanate. *J Alloys Compd*. 2017;711:400-405. doi:10.1016/j.jallcom.2017.03.361
33. Wu D, Ouyang L, Wu C, et al. Phase transition and hydrogen storage properties of Mg17Ba2compound. *J Alloys Compd*. 2017;690:519-522. doi:10.1016/j.jallcom.2016.08.159
34. Kumar S, Tiwari GP. Thermodynamics and kinetics of MgH_2-nfTa_2O_5 composite for reversible hydrogen storage application. *J Mater Sci*. 2017;52(12):6962-6968. doi:10.1007/s10853-017-0928-6
35. Ouyang LZ, Yang XS, Zhu M, et al. Enhanced hydrogen storage kinetics and stability by synergistic. *J Phys Chem C*. 2014;118:7808-7820.
36. Ouyang LZ, Yang XS, Dong HW, Zhu M. Structure and hydrogen storage properties of Mg3Pr and Mg3PrNi0.1 alloys. *Scr Mater*. 2009;61(4):339-342. doi:10.1016/j.scriptamat.2008.12.001
37. Zhu M, Wang H, Ouyang LZ, Zeng MQ. Composite structure and hydrogen storage properties in Mg-base alloys. *Int J Hydrog Energy*. 2006;31(2):251-257. doi:10.1016/j.ijhydene.2005.04.030
38. Ouyang LZ, Qin FX, Zhu M. The hydrogen storage behavior of Mg3La and Mg3LaNi0.1. *Scr Mater*. 2006;55(12):1075-1078. doi:10.1016/j.scriptamat.2006.08.052
39. Wikipedia. Ellingham diagram. Accessed 27 September, 2020. https://en.wikipedia.org/wiki/Ellingham_diagram
40. Itoh H, Fujii K, Nagasaka T, Hino M. Gibbs free energy and conditions of spinel ($MgO{\cdot}Al_2O_3$) formation in liquid steel. *Steel Res*. 2003;74(2):86-90. doi:10.1002/srin.200300165
41. Dolci F, Baricco M, Edwards PP, Giamello E. An investigation of the H_2 uptake in Mg-Nb-O ternary phases. *Int J Hydrog Energy*. 2008;33(12):3085-3090. doi:10.1016/j.ijhydene.2008.01.034
42. Nazir H, Batool M, Osorio B, et al. Recent developments in phase change materials for energy storage applications: a review. *Int J Heat Mass Transf*. 2019;129:491-523. doi:10.1016/j.ijheatmasstransfer.2018.09.126

How to cite this article: Jubair A, Rahman MA, Khan MMR, Rahman MW. Catalytic role of binary oxides (CuO and Al_2O_3) on hydrogen storage in MgH_2. *Environ Prog Sustainable Energy*. 2022;e13940. doi:10.1002/ep.13940